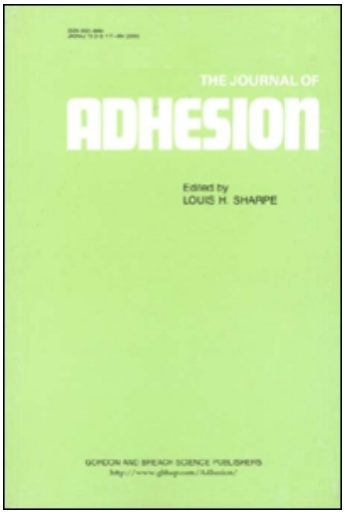

The Journal of Adhesion
Publication details, including instructions for authors and subscription information:
http://www.informaworld.com/smpp/title~content=t713453635

The Apparent Contact Angle of Liquids on Finely-Grooved Solid Surfaces-A SEM Study

J. F. Oliver[ab]; C. Huh[ab]; S. G. Mason[ab]
[a] Pulp and Paper Research Institute of Canada, Montreal, Canada [b] Department of Chemistry, McGill University, Montreal, Canada

To cite this Article Oliver, J. F. , Huh, C. and Mason, S. G.(1976) 'The Apparent Contact Angle of Liquids on Finely-Grooved Solid Surfaces-A SEM Study', The Journal of Adhesion, 8: 3, 223 — 234
To link to this Article: DOI: 10.1080/00218467608075085
URL: http://dx.doi.org/10.1080/00218467608075085

J. Adhesion, 1977, Vol. 8, pp. 223–234

Printed in Scotland

The Apparent Contact Angle of Liquids on Finely-Grooved Solid Surfaces—A SEM Study

J. F. OLIVER, C. HUH and S. G. MASON

Pulp and Paper Research Institute of Canada, Montreal, Canada, and Department of Chemistry, McGill University, Montreal, Canada

(*Received May 5, 1976*)

A finely parallel-grooved nitrocellulose surface has been employed as a model to study by scanning electron microscopy the influence of roughness on the spreading equilibrium of liquid drops. The Cassie and Baxter equation for spherical drops on a composite interface was experimentally confirmed with mercury and a similar equation derived for a cylindrical drop has also been shown to be approximately valid for liquid polyphenylether. The observed drop shapes have been explained and the importance of groove edges demonstrated.

Direct measurements of the microscopic contact angle of mercury locally on the grooved surfaces were found to be approximately the same for the smooth ungrooved surface.

List of symbols

A = drop cross-sectional area.
g = gravity.
h = depth of grooves.
$L_1; L_2$ = arc lengths of solid–liquid and liquid–void interfaces.
ΔP = pressure difference across drop surface.
r = contact line radius for a spherical drop; half base width for a cylindrical drop.
R = radius of drop.
S = drop cross-sectional circumference (for free surface).
x = width of ridges between grooves.
β = sessile drop shape parameter = $g\rho R^2/\gamma$.
γ = surface tension of liquid.
θ_0 = equilibrium and advancing contact angles on smooth surface (assumed equal).
θ_r = apparent contact angle.
θ_a = advancing θ_r.
θ_b = receding θ_r.
λ = wavelength of grooves.
ρ = liquid density.
ϕ = maximum slope angle of grooves.

I. INTRODUCTION

In a previous study[1] of the roughness effect using various model surfaces, we have shown that spreading equilibrium correlates reasonably with the measured roughness when the contact line remains almost circular. Subsequent scanning electron microscope (SEM) studies[2, 3] also showed the important role on spreading of local features of microscopic roughness, which may produce asymmetric spreading. This becomes particularly pronounced on parallel-grooved surfaces where for certain systems the liquid contact line may become very distorted and cylindrical drops are formed.

In an attempt to explore under what conditions such distorted drops are formed and how the apparent contact angle θ_r (defined in Figure 1(a) and (c)) correlates with the roughness parameters for them, we have made an *in situ* microscopic study on model parallel-grooved surfaces whose cross-sectional shape, depth h and wavelength λ were varied. Depending on the groove dimensions and the equilibrium contact angle θ_0 on the smooth surface, two limiting drop shapes were found: an almost spherical drop for liquids with large θ_0, as in the earlier work,[1] and an elongated cylindrical drop for small θ_0. For the almost spherical drop, we show from a mechanistic derivation rather than the conventional thermodynamic derivation, that the equation of Cassie and Baxter[4] is valid for parallel grooves. As we have cautioned earlier,[1] however, its general application to other surfaces is not warranted. For cylindrical drops, an equation relating θ_r with the roughness parameters is derived from a balance of interfacial forces. The validity of these two equations has been confirmed experimentally.

II. THEORETICAL PART

Approximate relations between the equilibrium contact angle θ_0 and apparent contact angle θ_r for spherical and cylindrical drops (representing two extremes of shape) on parallel-grooved surfaces can be derived by considering the balance of forces across a plane bisecting the drops (Figure 1).

i) *Spherical drop* Acting across the whole cross-sectional area A of the bisected drop, the capillary pressure $\Delta P = 2\gamma/R$ where γ is the surface tension and R the drop radius, is opposed by the surface tension force of the free liquid surface pulling over its circumference S normal to the cross-section (Figure 1(b)). In addition, there will be the horizontal component of γ acting on the solid locally along the contact line:

$$\Delta PA - \gamma S - \gamma L_2 + \gamma L_1 \cos\theta_0 = 0, \tag{1}$$

where L_1 and L_2 are the respective cross-sectional arc lengths of solid–liquid and liquid–void interfaces at the bisecting plane. The last term was obtained

utilizing the Stokes's theorem for the surface integral; a similar application has been made for the meniscus formed between two parallel circular cylinders.[5]

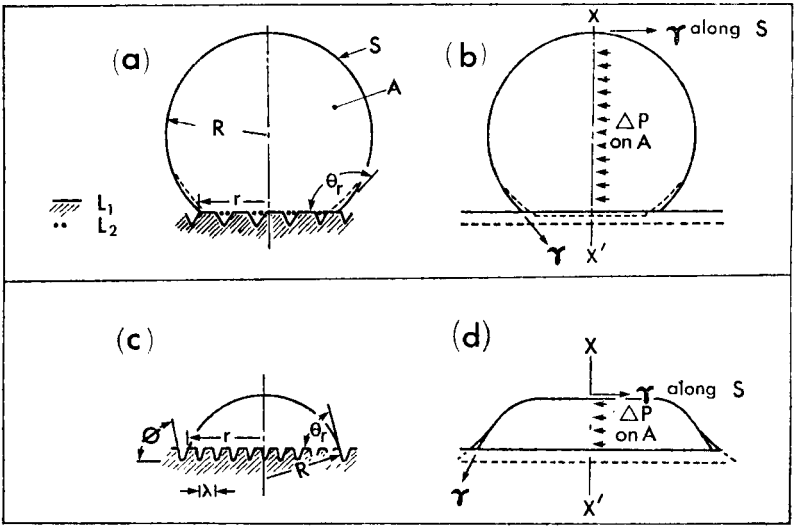

FIGURE 1 Equilibrium of liquid drops on parallel-grooved surfaces. (a) Cross-sectional view at the bisecting plane (shown by XX′ in (b)) of a spherical drop. For low-wetting liquids ($\theta_0 > 90°$), a composite surface is formed on the solid consisting of solid–liquid and liquid–void (dotted) interfaces. Broken lines at the drop profile indicate that the drop shape is not strictly spherical near the contact line. (b) Side view of the spherical drop. Broken lines indicate the contact line for the liquid–void interface and drop profile over the grooved areas. (c) Cross-sectional view and (d) side view of a cylindrical drop. For high-wetting liquids ($\theta_0 < 90°$) a non-composite surface is formed.

From simple geometry,

$$A = R^2(\theta_r - \sin\theta_r \cos\theta_r) \quad \text{and} \quad S = 2R\theta_r,$$

and inserting these into Eq. (1), we obtain

$$\frac{L_1}{2r}\cos\theta_0 - \frac{L_2}{2r} = \cos\theta_r \tag{2}$$

where $r = R\sin\theta_r$ is the contact line radius. We see that when $r \gg \lambda$, $L_1/2r$ and $L_2/2r$ become f_1 and f_2, respectively, and Eq. (2) becomes Cassie and Baxter's equation[4] for composite surfaces. For small drops for which r is comparable to λ, therefore, the Cassie–Baxter equation does not apply. If there is no void space ($L_2 = 0$), $L_1/2r$ becomes the conventional area ratio[6] $\bar{\sigma}$ for $r \gg \lambda$, and Eq. (2) reduces to Wenzel's equation.[7] We emphasize that the derivation of Eq. (2) (Cassie–Baxter equation for $r \gg \lambda$) was possible because the roughness consisted of *parallel* grooves. As we have discussed in

Ref. 6 it will apply only when the contact line can make reversible displacements without non-equilibrium jumps and hysteresis. The general application of the Cassie–Baxter equation for other surfaces is therefore not warranted.[8]

ii) *Cylindrical drop* If the drop is sufficiently elongated that its central portion can be taken to be cylindrical, then the capillary pressure $\Delta P = \gamma/R$, and from a consideration of the horizontal force balance (Figure 1(d)) similar to the above, the drop equilibrium is given by

$$\frac{L_1}{2r}\cos\theta_0 - \frac{L_2}{2r} = \frac{1}{2}\left(\cos\theta_r + \frac{\theta_r}{\sin\theta_r}\right), \tag{3}$$

where r and θ_r are as defined in Figure 1(c) at the drop cross-section. For the following experiments $L_2 = 0$, so that for $r \gg \lambda$, $L_1/2r \to \bar{\sigma}$. We see that Eq. (3) does not resemble the equation of Cassie and Baxter, or Wenzel.[7]

In the experiments described below, we test Eq. (2) for an advancing drop of a low-wetting liquid ($\theta_0 > 90°$), and Eq. (3) for a high-wetting liquid ($\theta_0 < 90°$).

III. EXPERIMENTAL PART

1. Procedure

a) *Preparation of surfaces* Parallel-grooved surfaces were prepared on smooth nitrocellulose phonograph record blanks (Audiodevices Inc., Glenbrook, Conn.) using an automatic disc recording machine (RCA Recording Studios, Montreal, Canada). Selected grooved and adjacent ungrooved areas were cleaned with a chemically neutral record cleaner (Lencoclean, Burgdorf, Switzerland) and then rendered conducting with a 300A film of aluminum in a vacuum evaporator.

b) *Drop deposition* i) *Spherical* After metallizing, the samples were exposed to atmospheric pressure and small drops of triply-distilled mercury were formed by splashing the liquid[9] over grooved and smooth areas (which served as a reference). Since under these conditions the aluminum film rapidly oxidized, the mercury did not amalgamate in the course of these experiments.

ii) *Cylindrical* Drops of an involatile polyphenylether (PPE) vacuum pump fluid (Santovic 5, Monsanto Chemicals) were deposited onto the surfaces from a syringe with a fine stainless steel needle (330 μm OD and 75 μm ID) mounted on a micro-manipulator. PPE has a viscosity of 22 poises and surface tension of 43 dynes/cm at 25°C.

After deposition of the liquid, samples were immediately examined in a Stereoscan Model 2A SEM (Cambridge Instruments, UK) at tilt angle[2] of about 90° and various SEM-graphs recorded.

(c) *Measurements of contact angle and surface roughness* SEM-graphs of selected spherical drops (0.15 to 0.45 mm dia.) and cylindrical drops (0.4 to 2.4 mm long, length/width ratio 2.0 to 4.5) viewed parallel to the groove direction, in a magnification range 125 to 650×, were used to measure: (i) the apparent advancing contact angle, θ_a; (ii) the equilibrium contact angle on the smooth surface θ_0; (iii) the contact line radius (or half the cylindrical drop width) r; (iv) the cross-sectional arc lengths of solid–liquid and liquid–void interfaces, L_1 and L_2; and (v) dimensions of the underlying roughness, viz. the wavelength λ and depth h of grooves, and width x of ridges.

The Bashforth–Adams's shape parameter[10] $\beta \equiv \rho g R^2/\gamma$ where ρ is the liquid density and g the gravity, was also calculated for the drops; for mercury, $\beta \leqslant 0.014$ and for PPE, $\beta \leqslant 0.026$, so that the gravity effect could be safely neglected.

Higher magnification SEM-graphs (1500 to 16,000×) were also used to measure the microscopic contact angle *in situ* on the grooved surfaces.[9]

The mean values of measured contact angles based on the left and right-hand sides of drop profiles were calculated and yielded an average deviation of $\leqslant \pm 2°$ for both liquids on all surfaces. Measurements of L_1, L_2 and r were estimated to be within $\pm 2\%$.

IV. RESULTS AND DISCUSSION

1. General observations

Deposited mercury drops assumed a near-spherical shape on all grooved surfaces (Figure 2) indicating that spreading was more or less uniform, whereas in the case of the much higher wetting PPE drops, spreading occurred along the grooves (Figure 3), resulting in cylindrical drops.

2. Effect of roughness on θ_a

Experimental data for the spherical and cylindrical drops are given in Table I along with values of θ_0 calculated from Eqs. (2) and (3). For mercury, the calculated value of $\theta_0 = 142.6 \pm 2.9°$ for drops traversing 1 to 7 grooves, and for PPE, $\theta_0 = 44.3 \pm 2.4°$ for drops traversing 6 to 18 grooves. These values are in good agreement with the respective measured values of θ_0 on the smooth (ungrooved) surface. In addition for mercury, direct observation of the local microscopic contact angle on the grooved surface at high magnification (Figure 4) confirmed that it was identical to the contact angle on the smooth surface θ_0. Similar observations on PPE were limited by its inferior conducting properties in the SEM.

Experimental values of θ_a are also plotted in Figure 5 with the corresponding theoretical curves from Eqs. (2) and (3). For a cylindrical drop, the

curve for Eq. (3) shows that θ_r is extremely sensitive to small changes in θ_0 and $L_1/2r$, as is evident from the experimental data given in Table I. Therefore, Eq. (3) can only provide an approximate estimate of θ_r. The minimum occurring in the curve at $\theta_r = 90°$ shows that a cylindrical drop is possible only when the condition

$$\frac{L_1}{2r}\cos\theta_0 - \frac{L_2}{2r} > \frac{\pi}{4} \tag{4}$$

is satisfied.

For spreading in the direction normal to the grooves, Shuttleworth and Bailey[12] proposed that drop advance ceased when $\theta_a = \phi + \theta_0$, where ϕ is the maximum local slope angle of the groove. This, however, will only apply when the liquid drop is truly cylindrical; otherwise, as is the case here with $\phi \sim 40°$, θ_a is much less then the predicted value due to the equilibrium

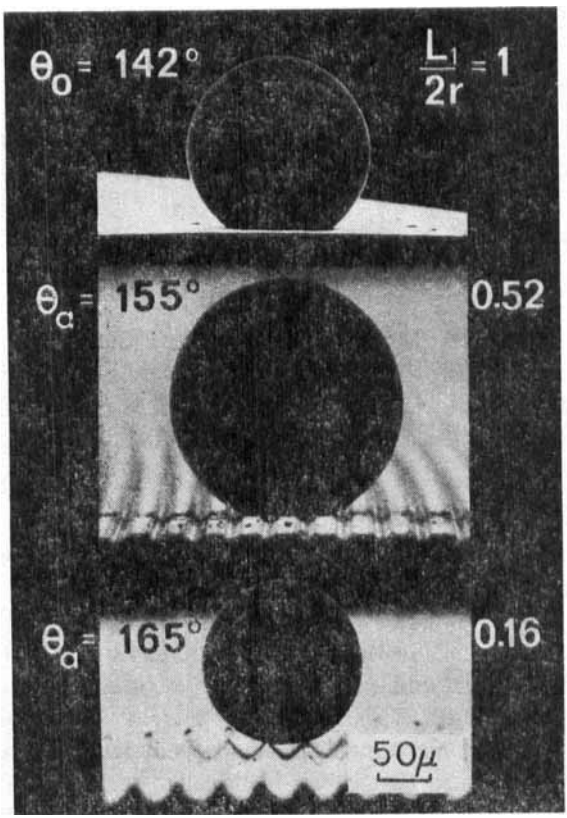

FIGURE 2 SEM-graphs of mercury drops on smooth and vee-grooved nitrocellulose surfaces. The drops are nearly spherical and as roughness increases, the apparent contact angle θ_r increases in accordance with Eq. (2). Note that the high value of θ_0 (142°) produces a composite interface on the grooved surface.

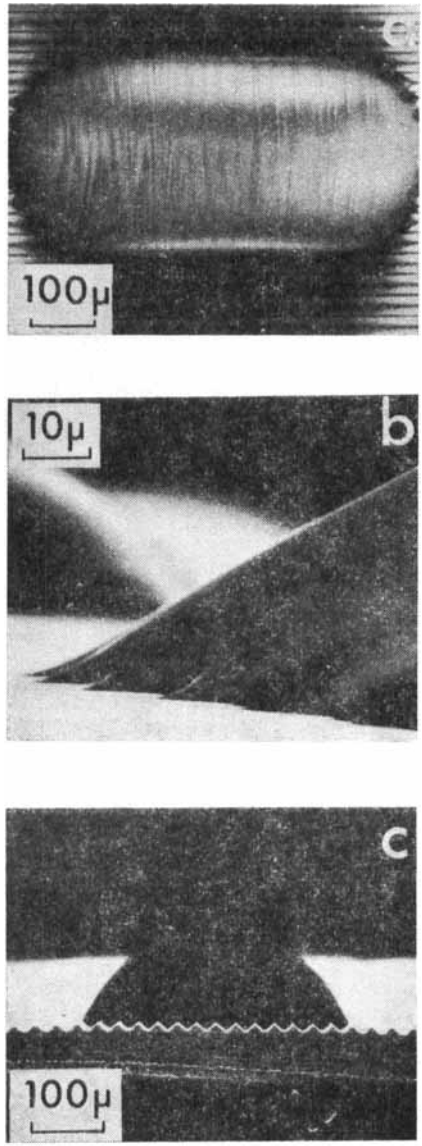

FIGURE 3 SEM-graph of a cylindrical PPE drop formed on a parallel vee-grooved nitrocellulose surface, viewed (a) from the top; (b) across the grooves; and (c) along the grooves. The elongation of the drop is the result of unhindered spreading along the grooves which serve as capillary channels, and inhibition of spreading across grooves due to the effect of edges.[11] Note the wrinkles on the drop surface in (b) compared with the smooth profile of (c); where the contact line protrudes in the grooves, the contact angle asymptotically approaches zero, whereas between the protrusions it is much higher.

condition, Eq. (3), which takes into account the spreading equilibrium along the grooves at each end of the cylindrical drop. The value of θ_a should also depend to some extent on the initial width of the deposited drop (thus the method of deposition), but this was not quantitatively examined in these

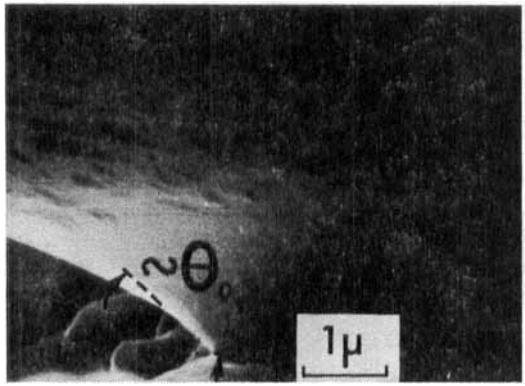

FIGURE 4 High magnification appearance of a mercury drop at the edge of a groove on a nitrocellulose surface. Note that within approximately 0.6 μm of the solid–liquid interface, the apparent advancing contact angle, θ_a reverts to a microscopically local angle, which is approximately equal to θ_0 on the smooth (ungrooved) surface.

TABLE I

Experimental data derived from SEM-graphs for approximately spherical mercury drops and nearly-cylindrical polyphenylether drops on parallel-grooved nitrocellulose surfaces

Liquid	No. of grooves traversed	λ (μm)	x (μm)	h (μm)	$2r$ (μm)	$L_1/2r$	$L_2/2r$	θ_a (deg.) meas.	θ_0 (deg.)[a] calc.
Mercury	1	21.0	1.5	7.5	22.5	0.13	0.87	166.0	140.2
	2	20.0	3.0	6.5	43.0	0.18	0.82	165.5	145.5
	3	20.0	4.0	5.5	67.0	0.26	0.74	163.0	146.5
	4	20.5	8.5	3.0	91.0	0.46	0.54	155.7	144.0
	4	20.5	8.5	3.0	91.5	0.48	0.52	152.5	140.0
	5	30.0	12.0	3.5	186.0	0.66	0.34	148.0	140.3
	6	32.0	20.5	2.5	224.0	0.67	0.33	147.0	139.2
	7	19.0	11.0	2.5	149.0	0.47	0.53	152.0	138.7
Polyphenyl-ether	13	33.0	2.5	13.5	450.0	1.30	0	22	40.7
	18	36.0	5.0	12.0	620.0	1.30	0	29	42.4
	11	33.0	3.0	14.0	354.0	1.30	0	39.0	44.5
	7	30.5	3.0	14.0	202.0	1.28	0	53.0	46.7
	14	28.0	2.5	11.0	372.0	1.29	0	56.0	48.0
	6	34.5	4.0	11.5	204.0	1.20	0	65.5	46.0
	13	33.0	8.0	9.5	400.0	1.22	0	69.0	47.5

[a] From [2] for spherical drops and [3] for cylindrical drops. The measured $\theta_0 = 142°$ for mercury and 43° for PPE.

experiments. We did observe, however, that immediately after deposition the drop rapidly traversed a certain number of grooves, and thereafter any additional increase in volume merely increased spreading along the grooves.

In the direction parallel to the grooves the ragged appearance of the contact line at the end of the drop (Figure 3(b)), was the result of capillary channelling in the grooves which produced tongues of liquid extending $\sim 15\ \mu m$ ahead of the drop; so that θ_a in this direction was less than θ_0, with its value approaching 0° at the plane of the smooth ridge. Also in some experiments, $\phi \simeq \theta_0$ corresponding to the condition of spontaneous wicking.[13]

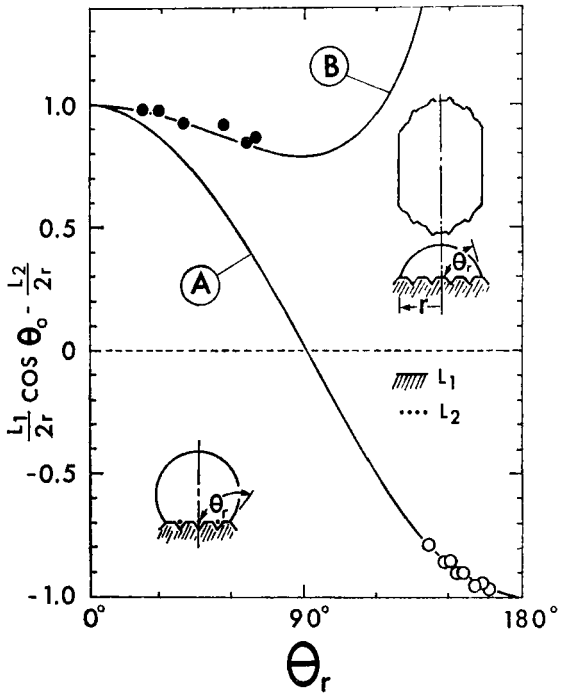

FIGURE 5 Measured values of the apparent advancing contact angle θ_a for approximately spherical drops of mercury (open points) and for nearly-cylindrical drops of PPE (closed points). The solid lines are calculated from Eq. (2) (curve A) and Eq. 3 (curve B). Note for curve A, when $\theta_r < 90°$, $L_2/2r$ becomes zero and Eq. (2) reduces to Wenzel's equation.[7]

For mercury for which $\theta_0 > 90°$, instead of capillary channelling, a slight dimple occurred in the contact line where the liquid–void interface ran underneath the drop. However, θ_a was approximately the same observed normal and parallel to the groove direction.

Although it may be possible to reduce the drop volume in the microscope[2] and form a receding drop, no attempt was made in these experiments in

view of the complications introduced by the edge effect.[1] Furthermore, according to Shuttleworth and Bailey[12] drop recession in the direction normal to the grooves ceases when the receding contact angle $\theta_b = \phi - \theta_0$, which for both liquids will be close to 0°.

3. Additional experiments

The groove edges played an important role in spreading on these surfaces. This was illustrated in some further experiments with mercury drops on surfaces with sinusoidal-like grooves. A comparison with the vee-grooves (Figure 6) showed that the edge effect[11] was lessened, and increased penetration of liquid into the grooves, while Eq. (2) remained approximately valid. Thus, although the roughness expressed as the area ratio of these surfaces was essentially the same, the slight difference in texture accounted for a significant modification in their behavior.

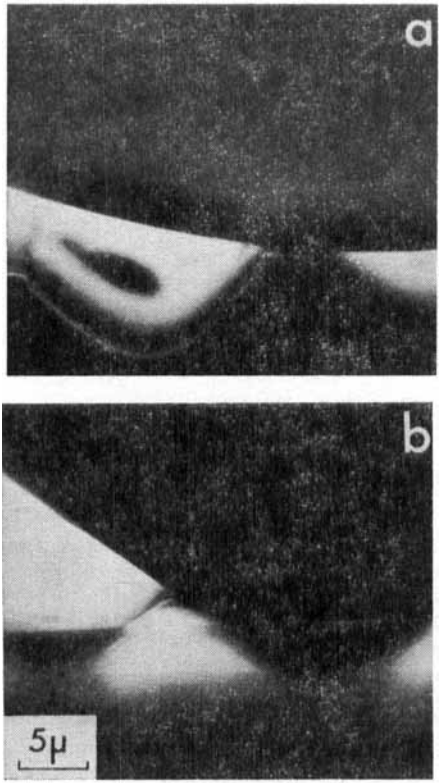

FIGURE 6 Comparison of the edge effect on the penetration of a mercury drop into: (a) vee-grooved and (b) sinusoidal-grooved nitrocellulose surfaces. Note the increased solid–liquid contact in case (b).

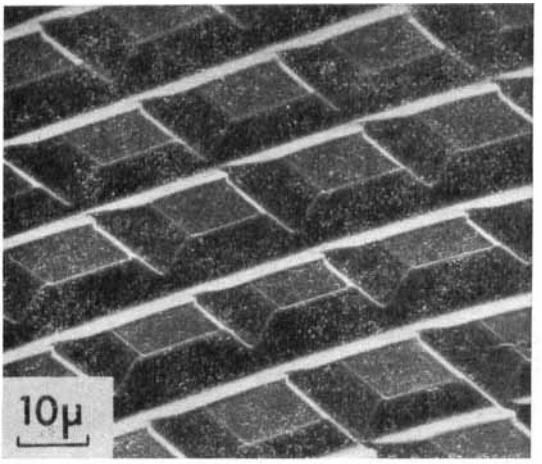

FIGURE 7 Parallel (approximately right-angled) cross-grooved nitrocellulose surface. Note the slight difference in the depth of grooves in one direction compared with the other, which produces a preferential spreading ($\theta_0 < 90°$) of liquid in that direction.

A surface consisting of parallel cross-grooves (Figure 7) was also briefly examined. Liquids with $\theta_0 < 90°$ also formed cylindrical drops despite a very slight difference in groove dimension, which produced preferential spreading along the direction of the deeper channels where capillary forces were greater. This further illustrates the dependence of the directional properties of spreading on surface roughness.

V. CONCLUDING REMARKS

Situations under which non-circular drops are formed on rough surfaces have been examined using the example of parallel grooves. The resultant spreading equilibrium was characterized approximately in terms of θ_a and various roughness parameters. Despite some inherent problems in utilizing the SEM technique, e.g. the accumulation of electrons by non-conducting liquids and metallizing the surfaces which modifies their surface free energy, these experiments confirm the validity of Cassie and Baxter's equation for spherical drops and Eq. (3) for cylindrical drops. Thus similar studies for other roughness textures are warranted.

We also confirmed in these experiments that the microscopic contact angle on the rough surface was equal to θ_0. Although this is generally assumed,[13] many surfaces are rough and chemically heterogeneous even at a microscopic level [2, 9] so that in practice the former may rarely apply. The role of these small-scale variations in surface roughness on the overall macroscopic spreading phenomenon therefore require further examination.

Acknowledgements

We are indebted to A. Rezanowich and G. Seibel of the Pulp and Paper Research Institute of Canada for their assistance with the scanning electron microscopy.

References

1. J. F. Oliver, C. Huh and S. G. Mason (in preparation).
2. J. F. Oliver and S. G. Mason, *J. Colloid Interface Sci.* (in Press, 1976).
3. J. F. Oliver and S. G. Mason, Proc. 5th Fund. Res. Symp. on Paper. Cambridge, U.K. (1973). British Paper and Board Ind. Fed. London.
4. A. B. D. Cassie and S. Baxter, *Trans. Farad. Soc.* **40,** 546 (1944).
5. H. M. Princen, *J. Colloid Sci.* **30,** 69 (1969).
6. C. Huh and S. G. Mason (in preparation).
7. R. N. Wenzel, *Ind. Eng. Chem.* **28,** 988 (1936).
8. R. H. Dettre and R. E. Johnson, *SCI Monograph* **25,** 144 (1967).
9. T. E. Hutchinson, *Thin Solid Films* **8,** R25 (1971).
10. F. Bashforth and J. C. Adams, "An Attempt to Test the Theories of Capillary Action" (University Press, Cambridge, England, 1883).
11. J. F. Oliver, C. Huh and S. G. Mason, *J. Colloid Interface Sci.* (in Press, 1976).
12. R. Shuttleworth and G. L. J. Bailey, *Disc. Farad. Soc.* **3,** 16 (1948).
13. R. H. Dettre and R. E. Johnson, in *Surface and Colloid Science*, Vol. 2, E. Matijevic, ed. (Wiley-Interscience, N.Y., 1969). P. 85.